

**Experimental Apparatus for Measuring
Ultralow Thermal Conductivity Structures**

by
Shiyi Liu

Mentor:

Austin J. Minnich

Assistant Professor of Mechanical Engineering

CALIFORNIA INSTITUTE OF TECHNOLOGY

Physics Senior Thesis

2012-2013

Experimental Apparatus for Measuring Ultralow Thermal Conductivity Structures

by
Shiyi Liu

Physics senior thesis submitted to the Department of Physics, May 8, 2013

Abstract

Ultralow thermal conductivity materials play an important role in many applications such as space exploration and thermal insulation. One of the primary challenges in studying heat conduction in these materials is performing basic thermal conductivity measurements, because even a small amount of steady heating results in enormous temperature increases. While methods do exist to measure the thermal conductivities of macroscopic materials, these techniques are difficult to apply to the microscopic samples that are the only samples available for some materials.

In this thesis, we describe an optical, non-contact experimental system for measuring ultralow thermal conductivities. The system we designed and built is a modified pump-and-probe system. With this system, we will be able to measure a sample as small as tens of microns without having physical contact between the tester and the sample. Different from a traditional pump-and-probe method, we used a pump laser with a very low repetition rate of a few hundred Hz, which can efficiently reduce the steady heating, and at the same time the transient heating is still enough to give a measurement result.

In the following chapters, we will first discuss the background of this thesis, including a brief introduction to the manufacture of the nano-lattice and the principles of the pump-and-probe method. Then we will go through some calculations done during the design process of the apparatus. Finally, we will present the test results from the experiments and compare them against the simulation.

Acknowledgement

Here I would like to acknowledge all the people who have helped me with this thesis. Without these people, much work in the thesis would not be possible. First, I am extremely grateful to my mentor, Professor Austin Minnich. Professor Minnich is very knowledgeable and diligent, and at the same time he is extremely kind and inspiring to his students. He always makes himself available to his students, in his office, in lab, and online. He is also very willing to discuss about my thesis, or other things. He has been giving suggestions and advices to my thesis regularly, and has spent many hours in lab helping me with my experiment. Most importantly, he has been very patient with me, especially with some of my trivial questions as well as mistakes because I did not have much background in his research area. I am very pleased and honored to get to know and to work with Professor Minnich in my last year at Caltech.

I would also like to thank Xiangwen Chen, who is a Postdoc working in the Minnich Group. Xiangwen has a great amount of experience with the pump-and-probe experiments, and has been very helpful and supportive to me. He has given many good suggestions to my experiment setup, and taught me a lot of things about the optical instruments in lab.

I also had a great collaboration with Lucas Meza, who is a PhD student from Greer Group. Lucas designed and created many nano-lattice structure samples for us, and taught me a lot about nanofabrication and other works Greer Group has been working on. He is also a very good communicator, as he regularly checks with me the progress we have made on our side.

I also have many thanks to the other members of the Minnich Group. I have built many friendships in the group and it has been my pleasure to get to know such a great group of people.

I am also grateful to Shawn Smith and his team from RPMC Lasers. They have offered us a lot of help when we were setting up the laser, and spent much time helping us troubleshooting the instrument.

I would also like to thank my advisor Dr. Kenneth Libbrecht, and Dr. Edward Stone from the Caltech physics department for offering me this opportunity to do a senior thesis.

Finally, I am very grateful to Zhao Liu, who gave me many good advices and supported me in many ways, and my parents, who have been very proud of and supportive to my work at Caltech, among many other things in my life.

Contents

- 1 Introduction and Background**
 - 1.1 Motivation for measurement system
 - 1.2 Principles of the Pump-and-Probe Method
 - 1.3 Organization of the Thesis
- 2 The Experimental System**
 - 2.1 Overheat of the Al Transducer
 - 2.2 Noise Calculation
 - 2.3 Optics
 - 2.4 Instrumentation
 - 2.5 Summary
- 3 Experiment and Data Analysis**
 - 3.1 Experiment Results
 - 3.2 Simulation and Data Comparison
- 4 Summary and Outlook**
 - 4.1 Summary
 - 4.2 Outlook and Conclusion

List of Figures

- 1-1 Nickel microlattices exhibit recoverable deformation
- 1-2 Nano-lattice structure created by the Greer Group.
- 1-3 Basic setup of a pump-and-probe experiment.
- 1-4 Sample arrangement for measuring the thermal conductivity of nano-lattice.
- 2-1 The relationship between the pump and probe beams in time.
- 2-2 A schematic of the essential component of the modified pump-and probe system.
- 2-3 The objective lens in the set up.
- 2-4 The pump laser pulses (tuned at 500Hz) viewed on an oscilloscope.
- 2-5 The pump laser from RPMC. 532nm, 5 μ J per pulse, pulse width 1.25 \pm 0.25ns, adjustable repetition rate, optimized at 100Hz and 5000Hz.
- 2-6 The controller for the pump laser.
- 2-7 The GUI of the computer software used to control the RPMC pump laser.
- 2-8 The probe laser used in the experiment set up. We collimated the output of the laser by using an aspheric lens.
- 2-9 Wearing an antistatic wristband can effectively avoid damaging the laser diode.
- 2-10 CCD camera used in the set up. We installed two lens tubes to block background light.
- 2-11 Image of the surface a glass sample as seen through the camera.
- 2-12 Thorlabs PDB210A large area balanced amplified photodetectors.
- 2-13 The LDC210C laser diode current controller.
- 3-1 Glass sample partially coated with Al transducer.
- 3-2 Sample mount and translation stage.
- 3-3 The probe beam (focused) as seen through the camera.

- 3-4 Matching the center of the pump beam to overlap with the center of the probe beam.
- 3-5 The surface of the Al coated glass sample seen through the camera.
- 3-6 Oscilloscope shows the detected signals collected in the pump-and-probe system.
- 3-7 A close-up view of one of the signals on the oscilloscope.
- 3-8 A Matlab simulation result.
- 3-9 Un-normalized curves.
- 3-10 Normalized curves.
- 4-1 Nano-lattice structure with a planer structure on the top.

Chapter 1

Introduction and Background

Pump-and-probe is a widely used method for studying thermal conductivity of materials, but when studying structures with ultralow thermal conductivity, a traditional pump-and-probe method is no longer a good choice. For test substrate with ultralow thermal conductivity, it is very difficult for the heat generated by the laser (usually with a repetition rate of 80MHz) to dissipate from the substrate, and as a result, the heat will accumulate quickly and will damage the sample. In this thesis, we designed and built a modified pump-and-probe system for measuring ultralow thermal conductivity structures. The unique feature we have in our pump-and-probe system is a pump laser with a low repetition rate (a few hundred Hz).

The inspiration for this thesis was a nano-lattice structure that was designed and manufactured by the Greer Group at Caltech. This lattice structure has very strong mechanical properties, and at same time it is very light. Another interesting fact is that it consists of about 1.3% of solid material, and 98.7% of air. Due to this high air-to-solid ratio, we also expect this structure to yield an ultralow thermal conductivity, and can be a good material used for thermal insulation. Possessing these contradicting properties, this nano-lattice can be potentially used in aerospace science, such as at atmospheric reentry.

Other methods do exist to measure ultralow thermal conductivity materials. For example, the hot wire method has been used to measure the thermal conductivity of aerogels [1]. Yet these techniques are only applicable to samples in macroscopic scale. The nano-lattice we saw from Greer Group was only $100\mu\text{m}\times 100\mu\text{m}\times 100\mu\text{m}$, which is too small to be measured with techniques that

require physical contact like the hot wire method. The pump-and-probe method, on the other hand, does not require any physical contact with the sample.

In the following sections, we will briefly provide an overview of the nano-lattice, which inspired us to propose this thesis, and is a good example of structures with ultralow thermal conductivity. Then we are going to go over the fundamental principles of the pump-and-probe technique.

1.1 Motivation for measurement system

In recent years, lightweight materials are becoming very popular in research as well as people's daily life: light materials reduce the total weight of the products, making things more portable, efficient, and pleasant to use. Although materials are weighting less nowadays, people still hope to maintain their strong mechanical properties. The ultralight metallic microlattice structure created by the Greer Group and HRL Laboratories in 2011 [2] is one of the materials that possess conflicting properties of being light and mechanically strong at the same time. This lattice structure can endure compressive strains of 50% without plastic deformation. Fig. 1-1 shows the pictures taken during the deformation test. Different from the traditional planer superlattice, this microlattice consists of a periodic array of hollow tubes that connect at nodes, forming an octahedral unit cell without any lattice members in the basal plane.

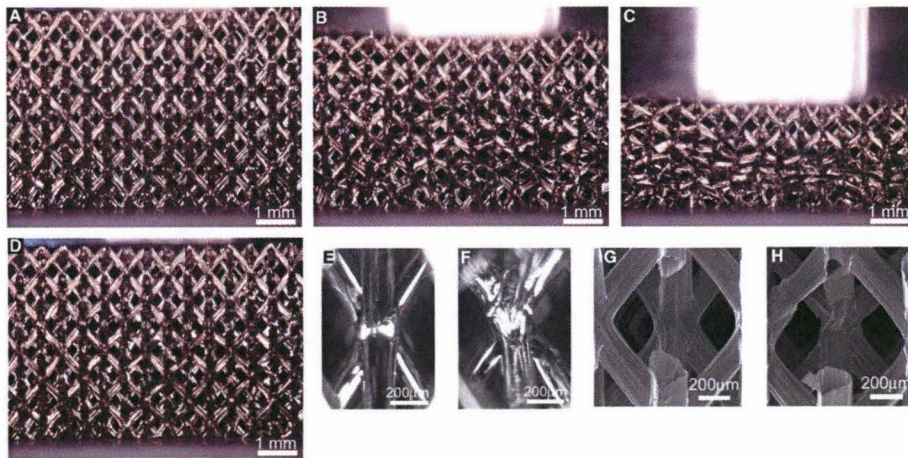


Fig. 1-1: Nickel microlattices exhibit recoverable deformation, taken from [2]
(A) Before deformation. (B) 15% compression. (C) 50% compression. (D) Full recovery after removal of load. (E) Optical image of unit cell unloaded. (F) Example of node buckling under compression. (G) SEM image of node before testing. (H) SEM image of node after six compression cycles at 50% strain.

Inspired by this microlattice structure, the Greer Group went further to look into the possibility of producing something similar in nano-scale. The manufacture of such delicate nano-lattice structure requires 3D printing with high precision.

The Greer Group is using a Nanoscribe *Photonic Professional* table-top lithography system to write the nanolattice (Fig. 1-2 shows this nano-lattice). This system is based on two-photon polymerization. This type of lithography uses a liquid resin that can be hardened under a focused laser beam. The reason that such printing technique is given the name “two-photon lithography” is because the monomers in the resin turn into solid only when they absorb the energy of two photons at once. Before this, 3D printing could only create solid structure on top of a previously created layer. Now, solid material can be created anywhere in the resin, which speeds up the printing process. It can also create many more structures that were previously difficult to make.

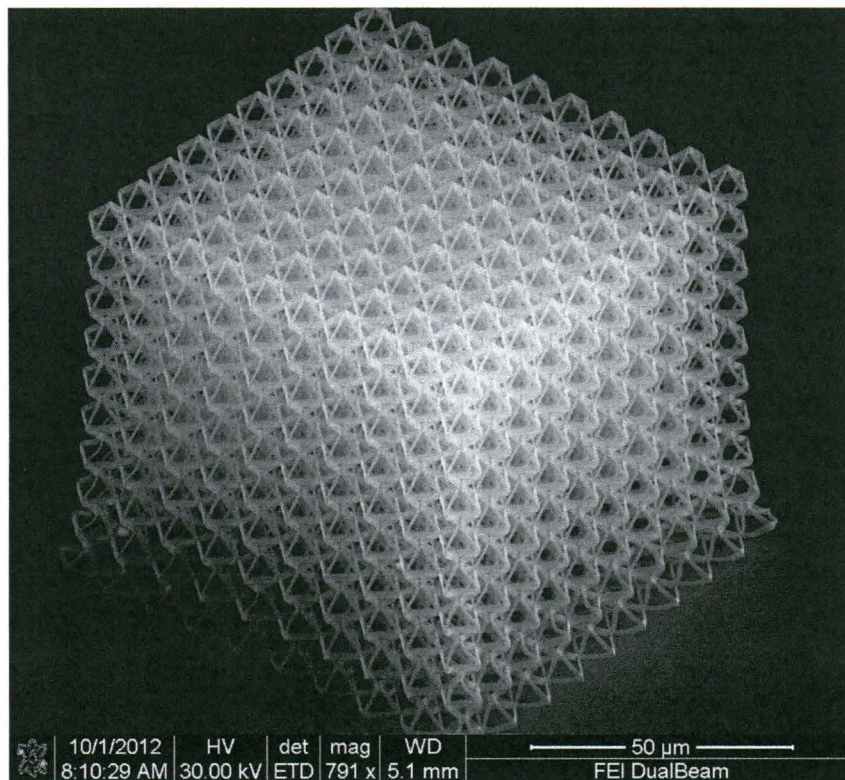


Fig. 1-2: Nano-lattice structure created by the Greer Group. Credit: Greer Group at Caltech.

This thesis will present a modified pump-and-probe system that can be used to measure structures with ultralow thermal conductivity, such as this nano-lattice structure. We have not yet measured the nano-lattice sample, but in this thesis, we will present the experiments done with a glass sample, which yields a relatively low thermal conductivity of about $1.05 \text{ Wm}^{-1}\text{K}^{-1}$ [3], compared that of Aluminum, which is about $237 \text{ Wm}^{-1}\text{K}^{-1}$ [4].

1.2 Principles of the Pump-and-Probe Method

Time-domain thermorefectance (TDTR) is a pump-and-probe technique that is commonly used to study the thermal properties, most significantly, the thermal conductivity, of materials on ultra fast time scale and micron length scale. This method can be applied to thin film material with thickness of a few hundred nanometers.

The pump-and-probe method is a very straightforward way of studying the excited state dynamics. This method consists of two stages. In the first stage, a pulse of laser, called the “pump” pulse, excites the material. This excitation heats up the sample, causing a small change in the thermorefectance. In the second stage, another laser pulse, called the “probe” pulse, arrives at the same area after a certain time delay to probe the state of the material. This time delay between the pump and probe pulses is usually controlled by a delay stage, which adjusts the optical path length difference between two laser beams. The change in the thermorefectance will lead to a change in the intensity of the probe signal received by the detector, and from there we will be able to study the thermal conductivity of the sample. A common pump-and-probe experimental setup is illustrated in Fig. 1-3.

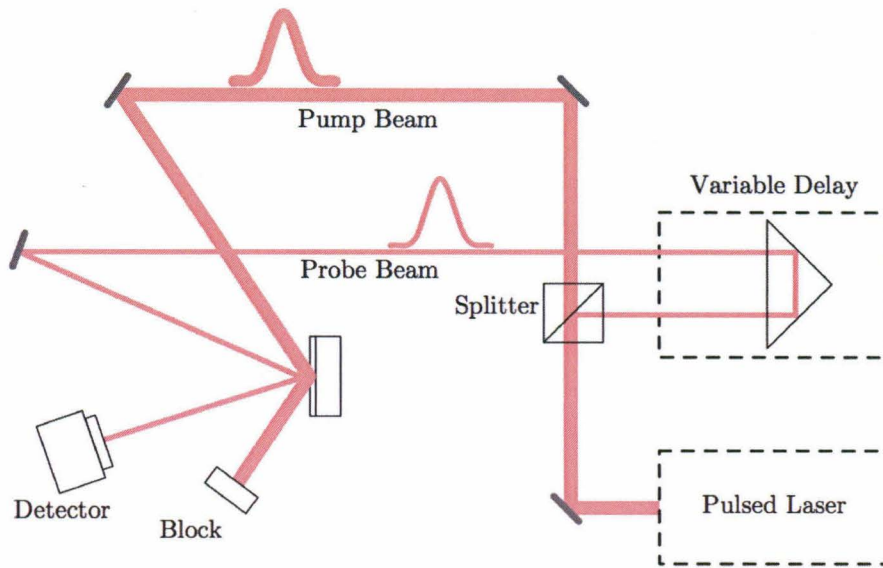


Fig. 1-3: Basic setup of a pump-and-probe experiment, taken from [6]

To prepare the sample used for the pump-and-probe technique, we need to have a layer of known material on top of the surface of the sample to serve as an optical transducer. In this thesis, we are using a thin film of Al (the thermal conductivity of Al is $237 \text{ Wm}^{-1}\text{K}^{-1}$ [4]) of thickness of about 100nm, and we measure the cooling process of this Al transducer. Fig. 1-4 demonstrates this configuration. When the pump laser hits the transducer, the heat will diffuse throughout the thin film. Within a hundred picoseconds, the heat will reach the surface of the sample, and increase the temperature of the sample in the local area by a few K. After this, the heat will continue traveling in the sample, cooling down the transducer film as phonons escape. The typical power used in a pump-and-probe experiment is within the range of 1mW to 100mW. This amount of laser power is good for measuring the thermal conductivity of many common materials; however, if the test sample possesses a very low thermal conductivity, we will have a problem due to steady heating. We will discuss this problem in Chapter 2.

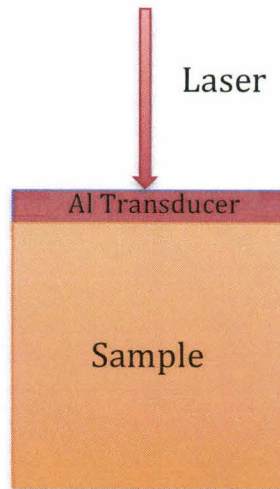


Fig. 1-4: Sample arrangement for measuring the thermal conductivity of nano-lattice.

1.3 Organization of the Thesis

This thesis consists of three parts. The first part, or Chapter 2, demonstrates the calculations we done for the design of the system. Then we will introduce the design and implementation of the pump-and-probe setup used in this thesis. This chapter contains all the details needed to reproduce our pump-and-probe system, including those of the optics, instrumentations, and so on. The second part, covered in Chapter 3, goes over the analysis of the data collected from the experiment. The third part, or Chapter 4, sums up this thesis, and provides a future outlook of the pump-and-probe method used in this thesis. We will also provide a brief update on the works done with the nano-lattice structure during the write up of this thesis.

Chapter 2

The Experimental System

In Chapter 1, we went over some basic principles of the pump-and-probe technique used in TDTR. This technique is a very common way of measuring thermal conductivity of materials, and in the past, many have modified the pump-and-probe method to study different substrates and to improve the accuracy of the measurement. Capinski and Maris [5], for example, developed an apparatus that uses a single-mode optical fiber after the delay stage to improve the accuracy of the measurement when the time delay of the probe relative to the pump is in the range above a few hundred picoseconds.

In this thesis, we propose a modified pump-and-probe method for measuring ultralow thermal conductivity structures. We will solve the problem of overheat by using a pump laser that has a much lower repetition rate than the one used in a traditional pump-and-probe experiment. In our experiment, we will use a pump laser with adjustable repetition rate, and we will set the repetition rate to about 500Hz. Lower repetition rate will give enough time between two consecutive laser pulses for the substrate to cool down, and protect the transducer from being burned. Another new feature in our system is that, unlike the typical pump-and-probe configuration shown in Fig. 2-1, we will be using a CW laser as a probe. The power of this CW laser is weak enough so we can test a glass sample without burning the transducer.

In this chapter, we will first go over the calculations done during the design process of the system, and then we will describe the design and implementation of the modified pump-and-probe system for measuring ultralow thermal conductivity structures.

2.1 Overheat of the Al Transducer

In this thesis, we modify the pump-and-probe system so to make it capable of measuring ultralow thermal conductivity structures, such as the nano-lattice. Ideally, only the pump laser will cause the temperature rise in the transducer and the sample. In reality, however, the probe laser will also heat up the sample. This heat might not be a crucial problem if we are measuring a common material, but when we are measuring a low thermal conductivity sample such as the nano-lattice, it will take a longer than usual time for the heat received by the Al transducer to escape into the lattice. In this situation, the heat from the laser will quickly accumulate in the transducer, and damage the transducer. To understand the possible result of this heating effect, we will calculate two things: first, the steady-state temperature rise in the sample due to the laser, and second, the amount of heat generated in the transducer due to its sudden exposure to a constant heat flux (probe laser).

First, we will study the steady-state temperature rise in the sample. By Eqn. (2.1) in *Analysis of heat flow in layered structures for time-domain thermoreflectance* by David G. Cahill [7], the steady-state temperature rise of the probed region of the sample can be estimated by the following equation:

$$\Delta T_0 = \frac{A_0}{2\sqrt{\pi}w_0\Lambda} \quad (2.1)$$

In which A_0 is the steady power absorbed by the substrate, w_0 is the $\frac{1}{e^2}$ radius of the laser beam, Λ is the thermal conductivity of the substrate.

Here we use the nano-lattice as an example of our test sample and see how much heat the steady-state heating will generate: we expect the thermal conductivity of a nano-lattice to be comparable to that of air, or $0.024 \text{ Wm}^{-1}\text{K}^{-1}$ [3].

In this case, if we take $A_0 = 2\text{mW}$ (a typical amount of energy absorbed by the Al transducer in a pump-and-probe experiment), $w_0 = 8\mu\text{m}$, $\Lambda = 0.024\text{ Wm}^{-1}\text{K}^{-1}$, for example, Eqn. (2.1) will give:

$$\Delta T_0 = \frac{2 \times 10^{-3} [\text{W}]}{2\sqrt{\pi} \times 8 \times 10^{-6} [\text{m}] \times 0.024 [\text{Wm}^{-1}\text{K}^{-1}]} = 2938.49\text{K} \quad (2.2)$$

This huge temperature rise will immediately vaporize the Al transducer, making the measurement impossible to perform. Regarding this issue, we proposed several solutions.

The first potential solution to this problem is to increase the radius of the probe laser beam, or the w_0 term in Eqn. (2.1), so that the energy is not as highly concentrated on one spot on the sample surface. If we maximize the radius of the probe laser beam to half of the length of the nano-lattice, or let $w_0 = 50\mu\text{m}$, Eqn. (2.1) will still give a fairly large result:

$$\Delta T_0 = \frac{2 \times 10^{-3} [\text{W}]}{2\sqrt{\pi} \times 50 \times 10^{-6} [\text{m}] \times 0.024 [\text{Wm}^{-1}\text{K}^{-1}]} = 470.158\text{K} \quad (2.3)$$

An acceptable temperature rise in a TDTR experiment is usually around a few K. Thus, we need to come up with another solution to decrease the temperature rise caused by the probe laser.

The second potential solution is to decrease the intensity of the laser beam, or the A_0 term in Eqn. (2.1). This seems to be the most straightforward solution to the problem, but decreasing the probe beam intensity will also decrease the signal to noise ratio, preventing an accurate measurement. Therefore, we have to seek for an alternative solution.

The third solution we proposed is to decrease the repetition rate of the laser beam from high frequency range (usually 80MHz) to a lower one, say, 100Hz. A lower repetition rate will give more time between two pulses for the transducer to cool down.

Fig. 1-5 shows the relationship between the pump and probe beams in time if the pump laser has a 100Hz repetition rate.

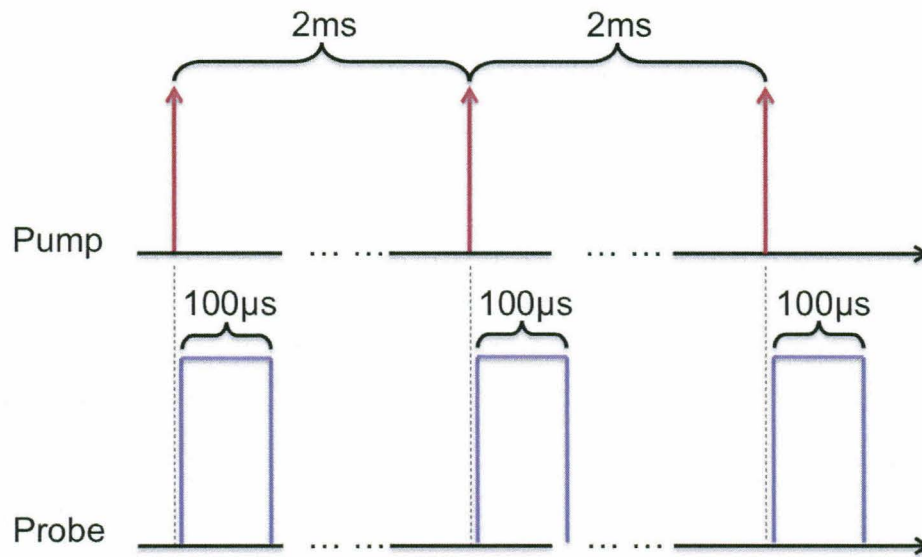


Fig. 2-1: The relationship between the pump and probe beams in time.

Now we can check the steady-state temperature rise with Cahill's equation (Eqn. (2.1)) again with a lower repetition rate. If we decrease the repetition rate so the power absorbed is decreased to $10 \times 10^{-6} \text{ W}$, we will only have a temperature rise of:

$$\Delta T_0 = \frac{10 \times 10^{-6} [\text{W}]}{2\sqrt{\pi} \times 50 \times 10^{-6} [\text{m}] \times 0.024 [\text{Wm}^{-1}\text{K}^{-1}]} = 2.35 \text{ K} \quad (2.4)$$

This temperature rise is acceptable for a pump-and-probe experiment, and the temperature rise will be even lower if we further reduce the repetition rate. If we use $10 \times 10^{-6} \text{ W}$ as a reference, at a repetition rate of a few hundred Hz, the appropriate pump power is around a few nJ per pulse.

Next we checked the temperature rise in the transducer due to sudden exposure to a constant heat flux. This equation is given by A. F. Mills in Eqn. (3.60) in *Basic Heat and Mass Transfer* [8] on page 170:

$$T - T_0 = \frac{q_s}{k} \left[\left(\frac{4\alpha t}{\pi} \right)^{1/2} e^{-x^2/4\alpha t} - x \operatorname{erfc} \frac{x}{(4\alpha t)^{1/2}} \right] \quad (2.5)$$

The temperature response on the surface of a material due to a sudden exposure to a constant heat flux at time $t = 0$ is given by $T - T_0$. In Eqn. (2.5), erfc is the complementary error function $\eta = 1 - \operatorname{erf} \eta$; q_s is the constant heat flux the surface is exposed to, with a unit of Wm^{-2} ; k is the thermal conductivity of the material, with a unit of $\text{Wm}^{-1}\text{K}^{-1}$; and α is the thermal diffusivity of the material, with a unit of m^2s^{-1} .

In our situation, we set $x = 0$ because we are interested in the surface of the Al transducer. Thus, Eqn. (2.5) becomes:

$$T - T_0 = \frac{q_s}{k} \left(\frac{4\alpha t}{\pi} \right)^{1/2} \quad (2.6)$$

We take the radius of the laser to be $50\mu\text{m}$, and the input probe power to be $192\mu\text{W}$ (this is the minimum probe power input we need to have a clear view of the signal on the oscilloscope; calculation can be found in the next section), which will give $q_s = 24446.2 \text{ Wm}^{-2}$. Let $k = 237 \text{ Wm}^{-1}\text{K}^{-1}$, $\alpha = 9.7 \times 10^{-5} \text{ m}^2\text{s}^{-1}$, $t = 100 \mu\text{s} = 10^{-4} \text{ s}$. In this case, $T - T_0 = 0.0115 \text{ K}$. This small temperature rise means the probe will only minimally heat the sample.

In this thesis, we wish to control the total temperature rise due to the heating effect of the laser beam to be less than or around 1K . From the rough estimations done above, we have a rough idea on the power of the lasers: the pump laser should carry around tens of nJ per pulse, and the CW probe laser should carry a few mW of power. (Notice that the reflectance of Al at 532nm is 0.92 , and that of Al at 800nm is 0.87 [9].)

2.2 Noise Calculation

Another issue we need to consider is the noise. In this thesis, we are going to collect the experiment data with an oscilloscope. In order to get a clear view of the signal, we need to take into account the noise of the system and estimate the minimum input signal needed to have a good measurement. This will not be a quantitative calculation, but this estimation will give us a good idea of how much input current the detector will need to receive in order to have a good measurement.

The potential noises in our experiment setup include: the noise from the detector (N_d), the noise from the laser (N_l), thermal noise, or Johnson Noise (N_t), and the noise in the oscilloscope (N_o). The following numbers were taken from a previous noise estimation done by Xiangwen Cheng in Minnich Lab:

$$\begin{aligned}N_d &= 0.3 \text{ mV} \\N_l &= 4 \text{ mV} \\N_t &= 0.037 \text{ mV} \\N_o &= 0.5 \text{ mV}\end{aligned}\tag{2.9}$$

In total, the noise from the system is about 4.8 mV. This is the minimum output voltage the detector needs to give in order to have a decent view on the oscilloscope. The corresponding minimum input current the detector needs to take in is given by:

$$I = \frac{Vn}{G}\tag{2.10}$$

Where G is the gain of the detector. In our case, we are using a Thorlabs PDB 210A Large-Area Balanced Amplified Photodetector, with a gain of 5×10^5 V/A [10]. Thus:

$$I = \frac{4.8 \times 10^{-3} [V]}{5 \times 10^5 [V/A]} = 9.6 \times 10^{-9} [A] \quad (2.11)$$

9.6×10^{-9} A, or 9.6 nA, is the minimum current input change the detector needs to detect in order to have a good view on the oscilloscope. The minimum power change the detector needs to detect is dependent of the responsivity of it.

The minimum power change needs to be detected is given by:

$$P_{\min} = \frac{I}{R} \quad (2.12)$$

Where R is the responsivity of the detector. From the Thorlabs website [10] we know that PDB 210A detector has a responsivity of $R = 0.5$ A/W at wavelength of 700nm. Plugging in the result from (2.11) and R into (2.12) gives a minimum power change of $P_{\min} = 1.92 \times 10^{-8}$ W.

This value is not yet very useful to us, because this power change is caused by a change in the thermorefectance of the Al transducer. We need one more step to estimate the amount of incident power we need to apply to the transducer in order to cause a power change of 1.92×10^{-8} W received by the detector. We are going to estimate the incident power through the following equation:

$$P_{\min} = P_{in} \times \beta \times \Delta T \quad (2.13)$$

In which P_{\min} is the result from Eqn. (2.12), $\beta = 10^{-4}$ K⁻¹ is the thermorefectance coefficient of Al, $\Delta T = 1$ K is the temperature change in the transducer, and P_{in} is the incident laser power. Re-arrange Eqn. (2.13) we get:

$$P_{in} = 0.000192W = 192\mu W \quad (2.14)$$

Thus, $192\mu\text{W}$ is an estimation of the minimum incident probe power needed to have a signal to noise ratio equal to 1.

2.3 Optics

Fig. 2-2 is a schematic that shows the essential components of our modified pump-and-probe system.

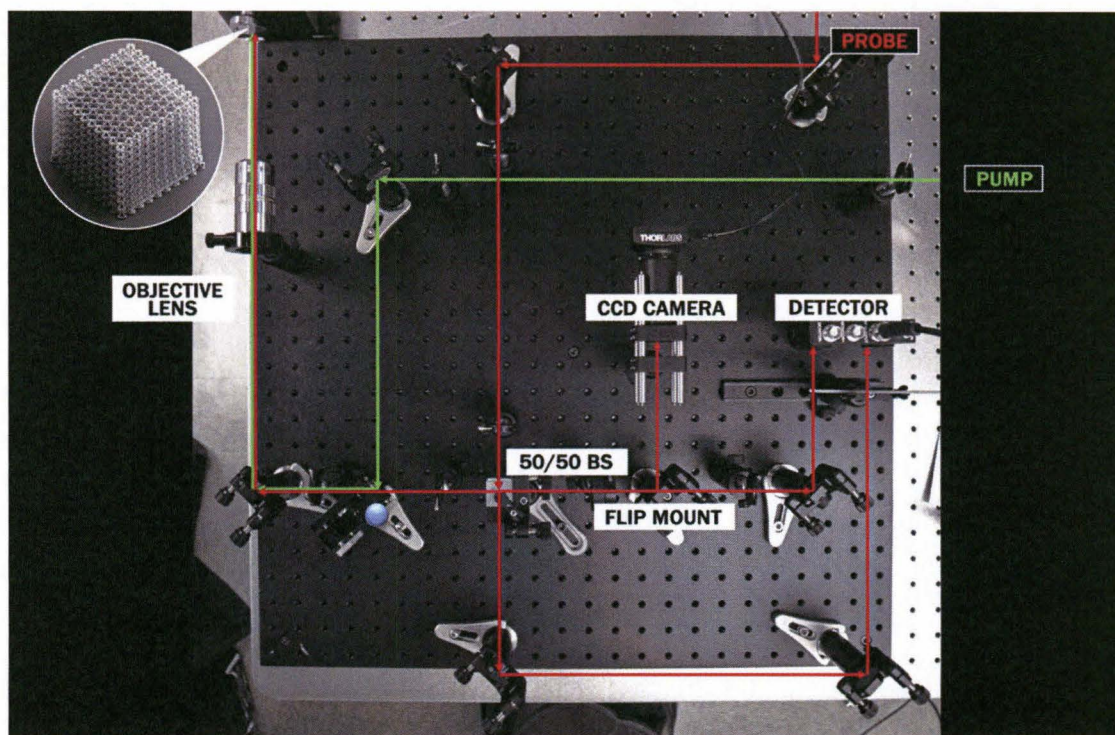


Fig. 2-2: A schematic of the essential component of the modified pump-and probe system. The probe beam goes through a 50/50 beam splitter; half of the probe beam will go to the balanced detector as a reference, and the other half of the beam will probe the sample. The flip mount shown in the schematic holds a silver mirror that can be flipped up or down so the laser beam bounces off the sample can either go into the camera or the balanced detector.

We are using silver mirrors (BB1-E03, 25.4mm diameter, broadband 750-1100nm) from Thorlabs to guide both the pump (532nm wavelength) and probe (785nm wavelength) beams. One flip mount is used in front of the CCD camera so that we can either choose to see the sample surface image on the computer (when the flip mount flips up) or the probe signal on an oscilloscope (when the flip mount flips down).

The pump beam gets reflected once on a cold mirror (marked with a blue dot in the schematic) before it goes to the test sample. The cold mirror is a dielectric mirror and a dichroic filter that let pass efficiently light with infrared wavelength, while reflects the light in the visible spectrum. In our system, this cold mirror can efficiently guide the pump beam to the test sample, while makes no impact to the light path of the probe beam.

The probe beam gets reflected twice after it comes out of the laser diode. Then it goes into a non-polarizing 50/50 beam splitter. A beam splitter splits a beam of light, in our case, into two halves. Fifty percent of the beam will reflect and the other half will transmit through. In our setup, after the beam splitter, one branch of the probe beam will go leftward, through the cold mirror then the objective lens, and onto the sample; the other branch of the probe beam will keep going down, and will eventually go into one of the two detectors in the balanced detector to serve as a reference.

Objective lens focuses the light rays to produce a real image. In our setup, we have a 10X objective lens with working distance of 33.5mm. This objective lens will focus both pump and probe beams to ensure that the cross section areas of both beam on the sample surface are less than 1mm. Fig. 2-3 is a close up picture of the objective lens in the setup. The black object around the objective lens is a ring light that was installed to better focus the CCD camera onto the sample surface when both lasers are off.

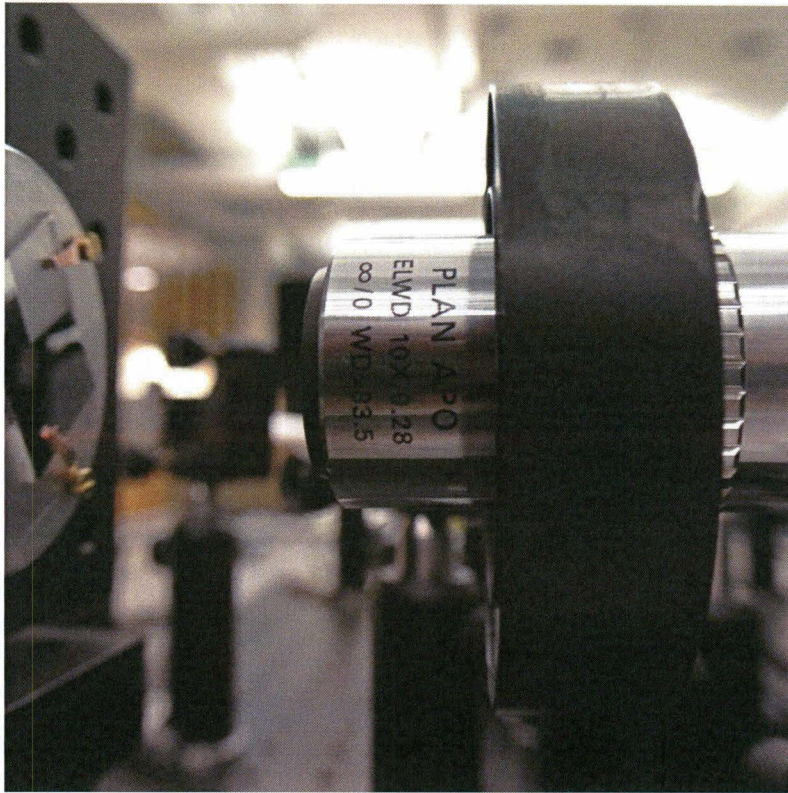


Fig. 2-3: The objective lens in the set up.

Fig. 2-4 shows the pump laser pulses viewed on an oscilloscope. The repetition rate of the laser is adjustable from a computer that has LaserComm V5.0 installed. (System requirement: Microsoft Windows 7) The laser (shown in Fig. 2-5) is connected through a controller (Fig. 2-6) to the computer through a USB port. The laser was made by RPMC, and the model is SP-532-5-5 (532nm, 5 μ J per pulse, pulse width 1.25 ± 0.25 ns, adjustable repetition rate, optimized at 100Hz and 5000Hz). In our experiment, we control the repetition rate of the pump laser through computer software. The GUI is shown in Fig. 2-7. The actual repetition rate shown on the oscilloscope is sometimes not exactly what we type in in the user interface. In Fig. 2-4, for example, although the computer software was suppose to output a series of 500Hz laser pulses, the real frequency we got was actually about 667Hz. But this frequency already gives enough time for the substrate to cool down.

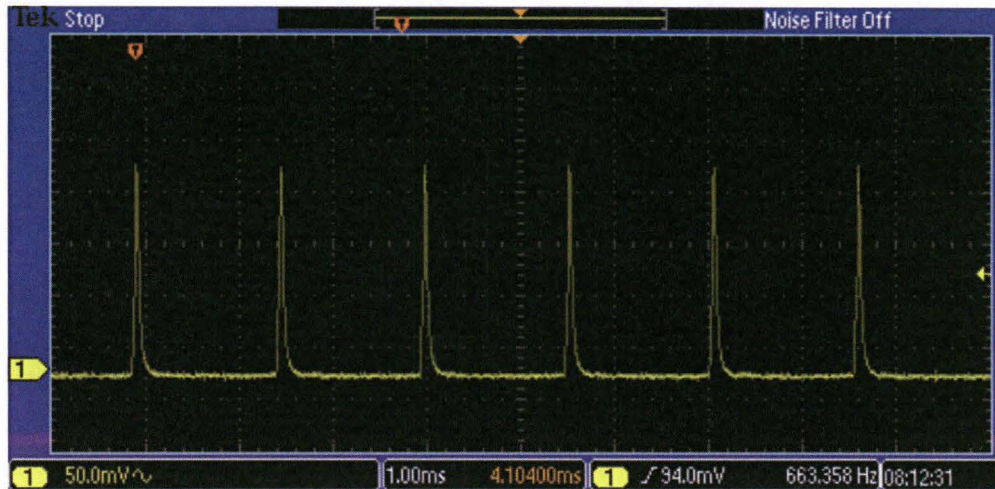


Fig. 2-4: The pump laser pulses (tuned at 500Hz) viewed on an oscilloscope. The actual frequency is slightly higher, about 667Hz, and this difference might be caused by the miscommunication between the GUI and the laser firmware.

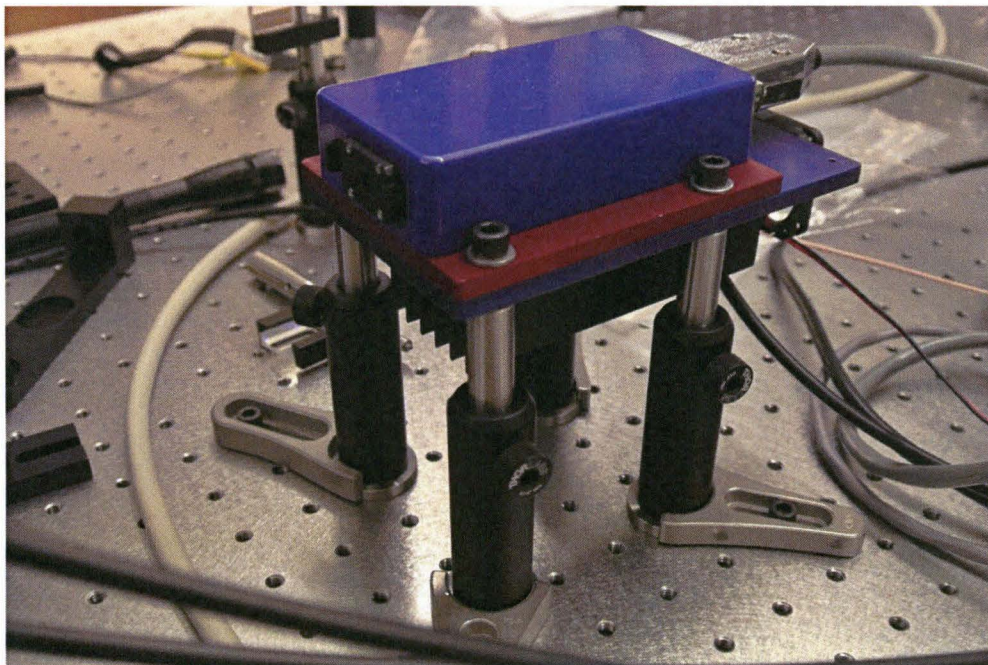


Fig. 2-5: The pump laser from RPMC. 532nm, 5 μ J per pulse, pulse width 1.25 \pm 0.25ns, adjustable repetition rate, optimized at 100Hz and 5000Hz.

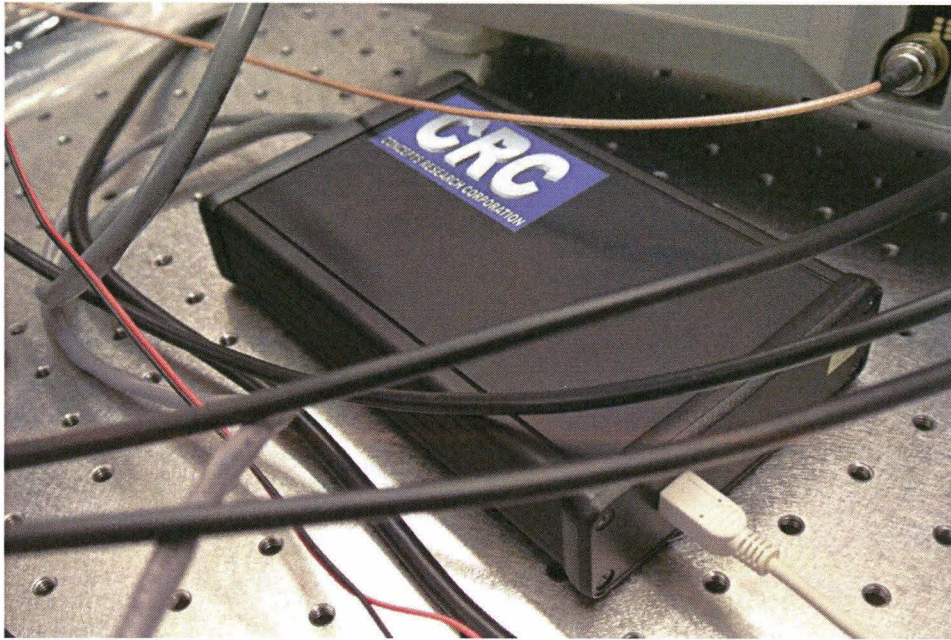


Fig. 2-6: The controller for the pump laser. This controller is connected between the computer and the laser. It is also possible to externally trigger this controller to control the laser directly, instead of through the computer software. The former way of controlling may give a more stable and accurate result.

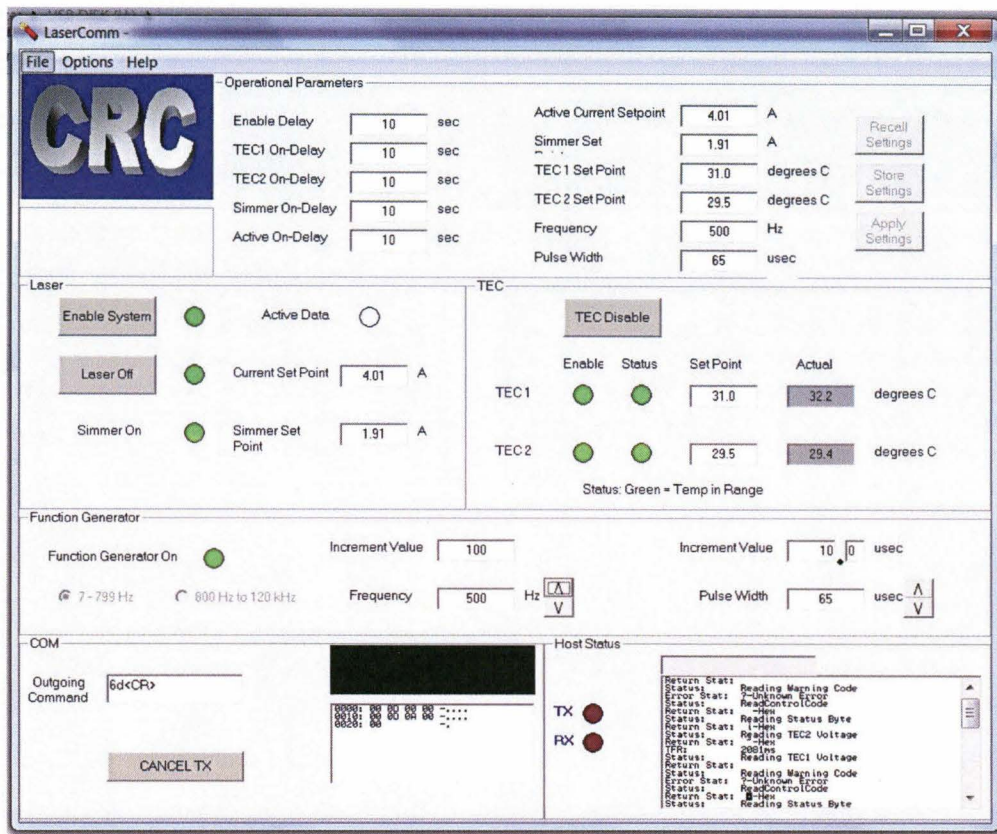


Fig. 2-7: The GUI of the computer software used to control the RPMC pump laser.

This software is run in Microsoft Windows 7 environment.

The probe laser is a Thorlabs 785nm laser diode (QL7816S-B-L) with 25mW power, 5.6mm diameter, and B pin code. We mounted this laser diode into a Thorlabs LDM21 laser diode temperature controlled mount. The output of this laser diode is highly divergent, so collimating optics is necessary. In our set up, we collimated the laser diode output by using a mounted aspheric lens (Thorlabs C230TME-B) with focal length of 4.51mm (the actual working distance was 2.92mm), numerical aperture of 0.55, broadband AR coated, and designed for 600-1050nm wavelength. This aspheric length was mounted onto LDM21 through a Thorlabs S1TM09 SM1 to M9×0.5 lens cell adapter. Assembling all these parts together, we get the probe laser, as shown in Fig. 2-8.

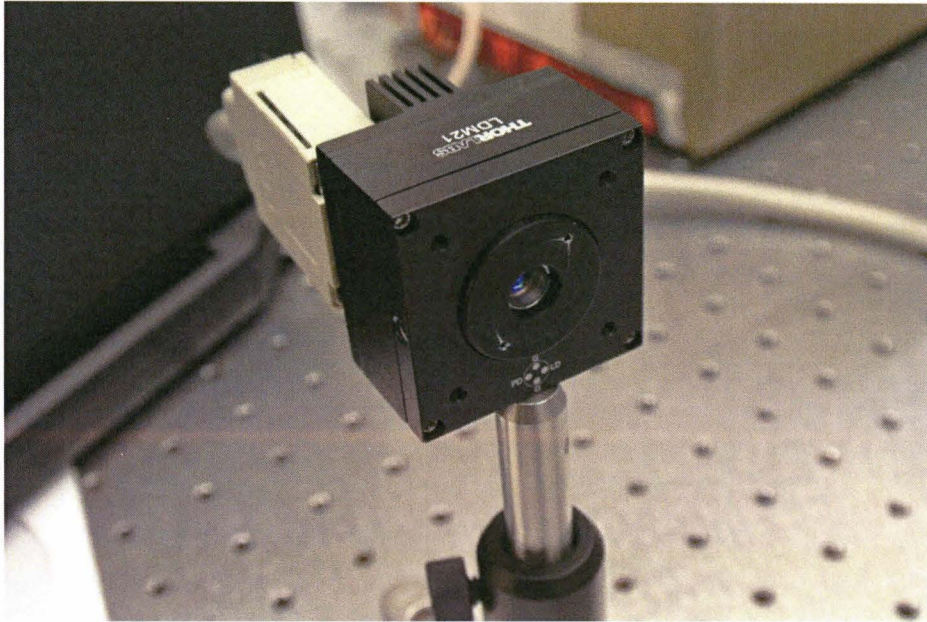


Fig. 2-8: The probe laser used in the experiment set up. We collimated the output of the laser by using an aspheric lens.

Another fact about the laser diode is that it is electrostatic sensitive, and so it can be easily damaged by common static charges. Wearing an antistatic wristband (Fig. 2-9) is a very effective way of avoiding this damage.

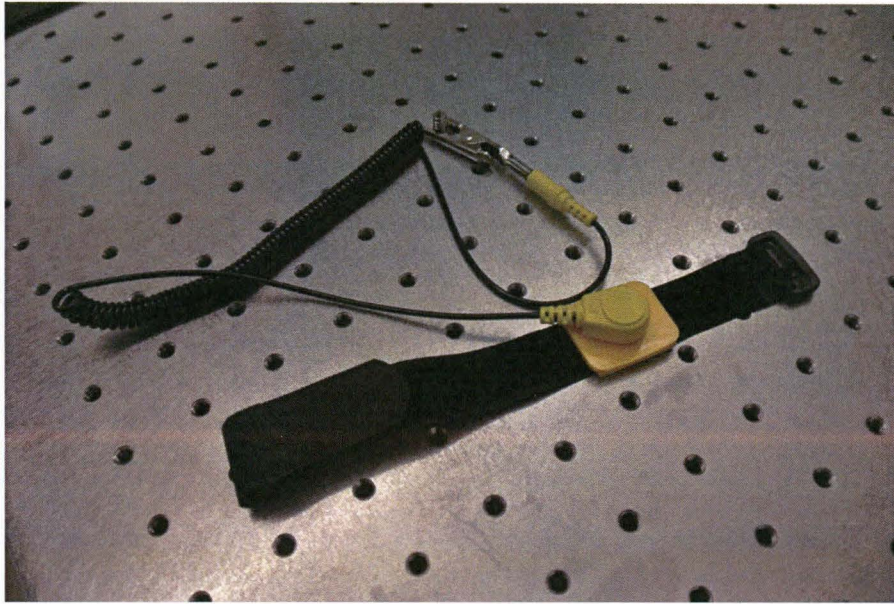


Fig. 2-9: Wearing an antistatic wristband can effectively avoid damaging the laser diode.

Besides the main components mentioned above, we also installed before the cold mirror two plano-convex lenses (Thorlabs LA1422-B, with 25.4mm diameter, 40.0mm focal length, B coated) to shrink the pump beam, which diverges greatly as it reaches to the sample.

In addition to its divergence, the pump beam is also too strong for the experiment. In order to reduce its power, we tried several ND filters on its path. After several tries, we found out that Thorlabs ND10A and Thorlabs ND04A are the appropriate ones for the experiment. In Chapter 3 we will talk more about how these two ND filters were used in the experiment.

Another optical instrument we installed is a plano-convex lens (focal length 250mm) before the camera. This lens focuses the probe beam before it goes into the camera.

Optical experiments in general are very precise. The optical instruments in our setup require very precise alignment. Good alignment is usually crucial in getting accurate data. In addition, however, we also need to have a good

understanding on the electronic part of the experiment. In the next section, we will go over in details the electronic instruments we used in the set up.

2.4 Instrumentation

The main electronic components in our set up include: one CCD camera, one large area balanced detector, and one laser diode controller.

Fig. 2-10 shows the camera in the set up. This is a Thorlabs CCD camera (DCC1545M high resolution USB2.0 CCD camera, 1280×1024 resolution, with monochrome sensor). We also installed two lens tubes to block background light. By flipping the flip mount up, we will be able to direct the probe beam into the camera. We use this camera to see the sample surface, and also to check whether the pump and probe lasers are on focus. We used UC480 Viewer (downloadable from Thorlabs website) to control the camera and to see the image on a computer. Fig. 2-11 is a glass sample surface seen through the camera.



Fig. 2-10: CCD camera used in the set up. We installed two lens tubes to block background light.

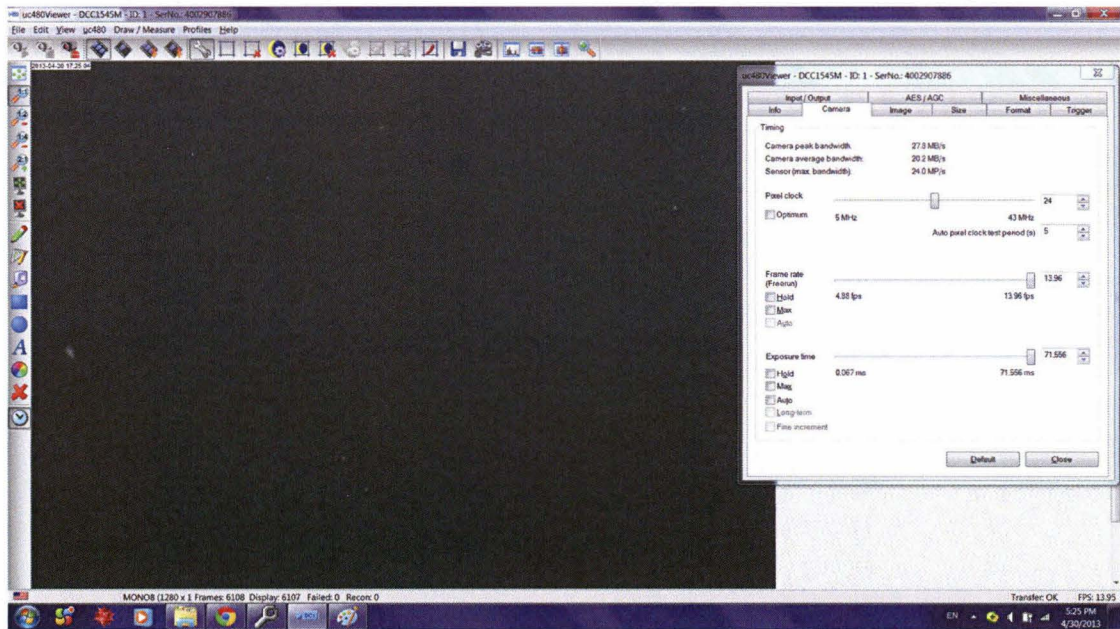


Fig. 2-11: Image of the surface a glass sample as seen through the camera.

For this thesis, we used a Thorlabs large area balanced amplified photodetectors (PDB210A, 320-1060nm) for detection. This balanced detector (shown in Fig. 2-12) consists of two well-matched large-area photodiodes and an amplifier that generates an output voltage proportional to the difference between the photocurrents in the two photodiodes, which come from the optical input signals received by the two detectors. In our situation, in Fig.2-2, the optical signal received by the detector on the right is half of the original probe beam, which serves as a reference in the experiment. The optical signal received by the detector on the left is the probe beam bounces off the sample.



Fig. 2-12: Thorlabs PDB210A large area balanced amplified photodetectors. Taken from Thorlabs's website.

In our experiment, the balanced detector is used to detect the probe beam. However, the back reflection of the pump beam is also partially going into the detector. To block these incoming pump beam, we installed one filter (FELH0750 Premium Longpass Filter, Cut-On Wavelength: 750nm) on each photodetector in PDB210A. By using these two filters, we can ensure that the detector is not detecting the pump signals.

As mentioned previously in the optics section, we used a Thorlabs laser diode as the probe beam. To drive this laser diode, we used Thorlabs benchtop LD

current controller (LDC210C, ± 1 A HV). This laser diode current controller has laser current range from 0 to ± 1 A. The laser diode we have for this experiment (QL7816S-B-L) has an average operating current of 45mA, and min/max operating current of 30mA/60mA. Thus, the LDC210C benchtop controller is efficient. Fig. 2-13 shows the LDC210C laser diode current controller we have for the experiment.

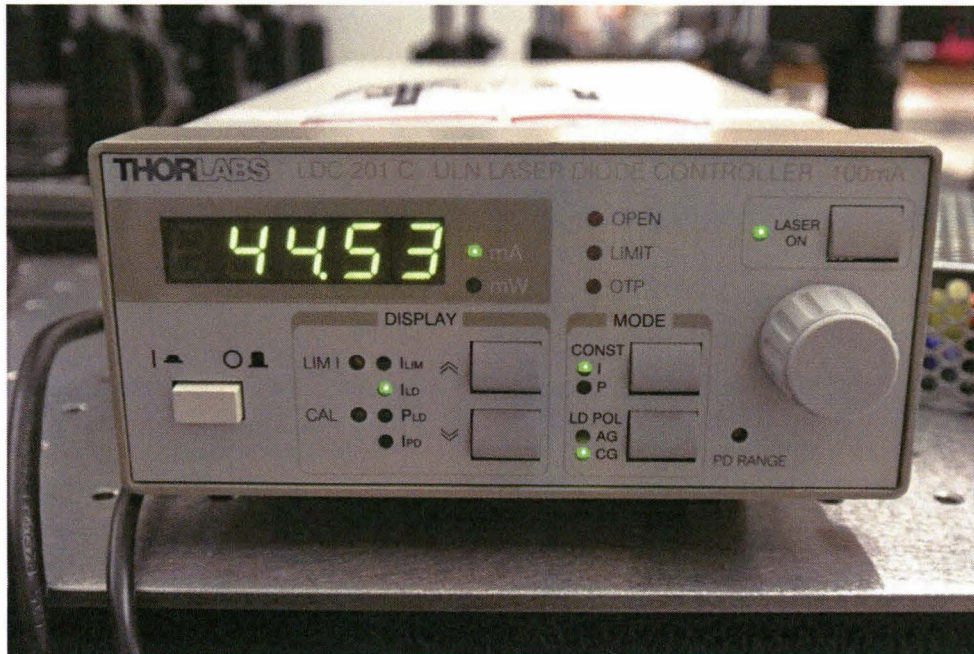


Fig. 2-13: The LDC210C laser diode current controller.

In addition to these main electronic components, we also used a beam profiler to check the beam shape and quality, and a power meter to check the output power of the lasers at different point of the set up.

The beam profiler we have is the Thorlabs BP104-UV beam profiler.

The power meter we have is a Thorlabs PM100D digital handheld laser power and energy meter.

2.5 Summary

In the previous part of this chapter, we have gone over all the details of our experiment setup. The principles behind our setup are very similar to those of most of the other pump-and-probe systems built by others. One unique feature in our setup is that we are driving the pump laser at an ultra-low frequency (a few hundred Hz), while a common pump-and-probe system usually has an ultra-fast pump laser driven at 80MHz. The reason that we are having a much lower repetition rate was discussed in details in the previous chapter: we are modifying the pump-and-probe system so that it is capable to measure some materials with ultra-low thermal conductivity without overheating and damaging the transducer.

Chapter 3

Experiment and Data Analysis

In this thesis, we built a modified pump-and-probe system that has a pump laser driven at very low frequency (a few hundred Hz). This system was designed to measure ultralow thermal conductivity of materials such as the nano-lattice.

The sample material we used to test this modified pump-and-probe system is a piece of Al coated glass sample. Fig. 3-1 shows the glass sample (partially coated with Al transducer) we used.

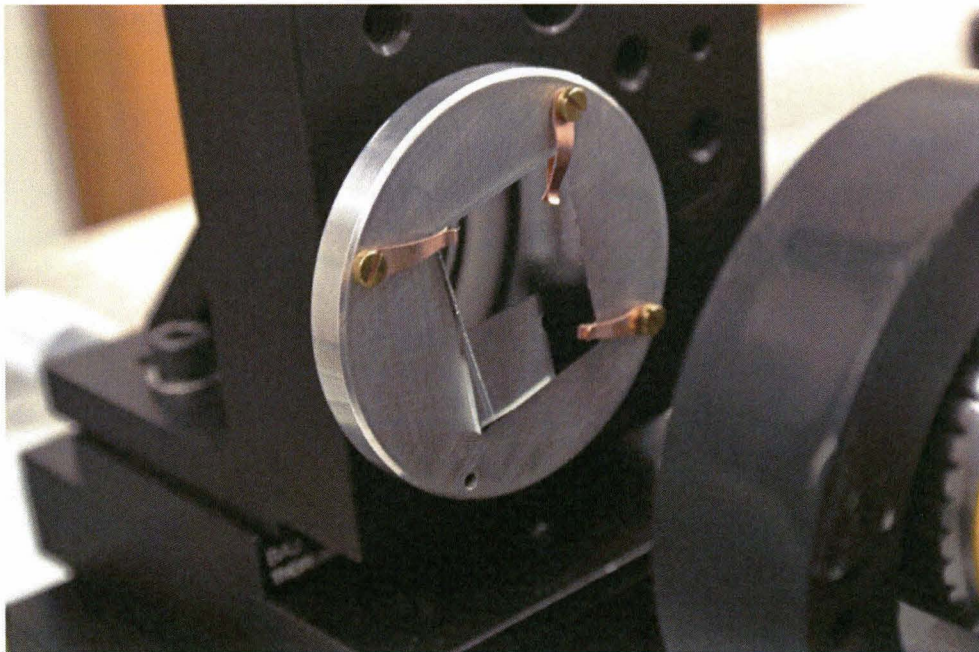


Fig. 3-1: Glass sample partially coated with Al transducer. The transparent part is not coated. All the measurements we have done for this thesis were done on the part with Al coating.

The most important step in the testing is to focus and overlap both pump and probe beam (or at least make sure that the probe beam is focused), by looking at the sample surface through the camera and adjusting the distance between the sample and the objective lens. This distance can be adjusted by turning the knob on the translation stage, shown in Fig. 3-2.

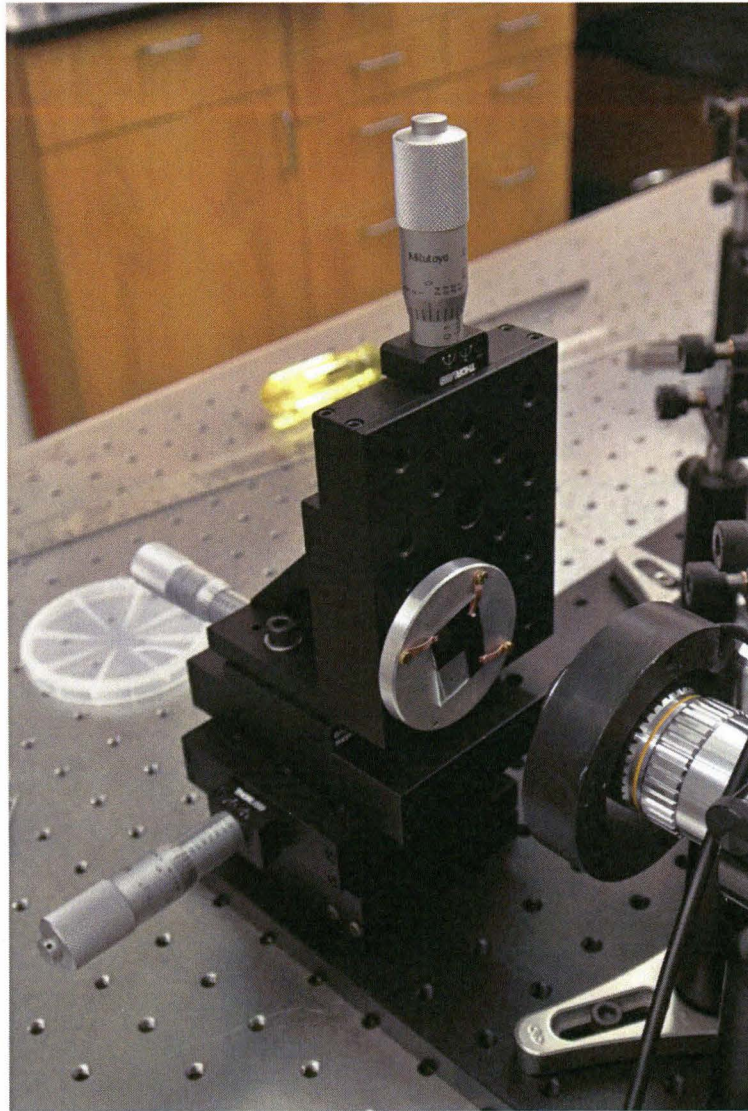


Fig. 3-2: Sample mount and translation stage. This stage has three knobs, controlling the position of the sample in all three directions.

To focus the beams, we first block both pump and probe beams, and turn on the ring light, which lights up the sample surface. Next we adjust the camera position so that we can clearly see the sample surface. When everything is in focus, we should be able to see the scratch marks on the sample surface, like the white spots shown in Fig. 2-11. Then we turn off the ring light, and unblock the probe beam. At this moment, it is most likely that the probe beam will be out of focus. Now we need to adjust the knob on the translation stage so that the probe beam is focused. To focus the pump beam, we do the same thing by adjusting the knob on the stage until the image of the pump beam is clear. It usually happens that the pump and probe beam are focused on different plane. In this case, we at least need to make sure that a beam is focused when we are marking its position, because only then will we be able to see the real position of the image through the camera.

To overlap both laser beams, we use the probe beam as the reference and only adjust the position of the pump beam, because changing the probe beam will change its light path into the detector and camera. We first find the probe beam through the camera, and mark the position on the screen (Fig.3-3).

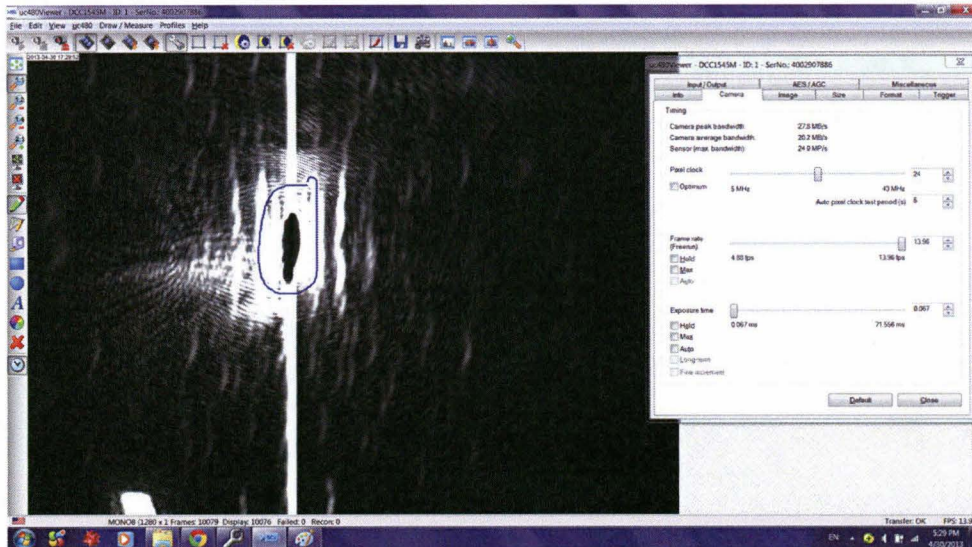


Fig. 3-3: The probe beam (focused) as seen through the camera. The blue circle was drawn to mark the approximate position of the center of the probe beam.

We then block the probe beam, and unblock the pump beam. Turn the knob on the transition stage to make it focused. Next, use the blue circle we previously drawn as a reference, and turn the knobs on the lens mount that holds the cold mirror to move the pump beam until the center of it overlaps the center of the probe beam (Fig. 3-4).

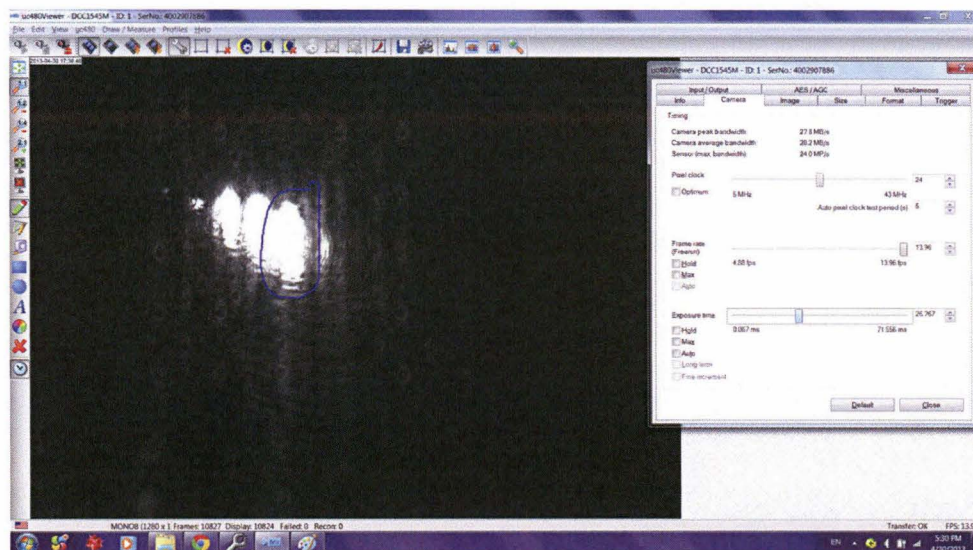


Fig. 3-4: Matching the center of the pump beam to overlap with the center of the probe beam. The blue circle marks the approximate position of the center of the probe beam.

When the overlapping is done, block the pump beam again and unblock the probe beam. If it is difficult to focus both the pump and probe beams on the same plane, we need to have at least the probe beam on focus, so we can have a good measurement. By adjusting the knob on the translation stage once more, we move the sample to the position where the probe beam is focused.

One last thing to do before we take a measurement is to flip the flip mount down and guide the probe beam into the balanced detector.

3.1 Experiment Results

In this thesis, we used an oscilloscope to acquire and store the data. The oscilloscope we used was a Tektronix DPO 2014B Digital Phosphor Oscilloscope (100MHz, 1GS/s).

The balanced detector has three output that can be connected to three channels on the oscilloscope through BNC cables, as can be seen in Fig. 2-12. In our experiment, Channel 1 of the oscilloscope is connected to the pump laser itself, so what we see in Channel 1 is the original laser pulses directly from the pump laser. Channel 2 and 3 of the oscilloscope are connected to the MONITOR+ and MONITOR- of the balanced detector. These two channels show the input signal from the two detectors in the balanced detector. Channel 4 is connected to the RF OUTPUT of the balanced detector. The voltage in this output is proportional to the difference between the photocurrents in the two photodiodes (MONITOR+ and MONITOR-). As we have discussed in Chapter 1, the change in the thermorefectance of the sample causes the change of the intensity of the reflected probe laser beam, which, eventually, is represented by a change of voltage that can be seen on the oscilloscope. The signal in Channel 4 is the result after subtracting the signal bounced back from the sample from the reference probe signal (recall that the original probe beam was split into two halves: one of them reaches to the sample surface, while the other half goes directly into the detector).

After connecting the balanced detector to the oscilloscope, we can start to look for the signals. If we are unable to detect any signal, it might imply bad overlapping of the pump and probe beam. To solve this problem, we carefully adjust the angle of the cold mirror until we see the signals. Another thing to keep in mind is that the pump beam might damage the transducer if we don't have the appropriate filter in the light path. Once the surface is damaged, we will not be able to see any signal in Channel 4.

To decrease the laser power, we used ND filters, or neutral density filters. A ND filter reduces the intensity of all wavelengths of light equally, giving no changes in other properties of the light.

At first, we ran the experiment without using any ND filter. In this situation, we weren't able to get any data, even after ensuring that the pump and probe beams were overlapping. We then blocked both the pump and probe beam, and looked at the sample surface with the camera with the ring light on. Under the camera, we could clearly see that the high power laser had burned the transducer. Fig. 3-5 was what we saw before (on left) and after (on right) the damage.

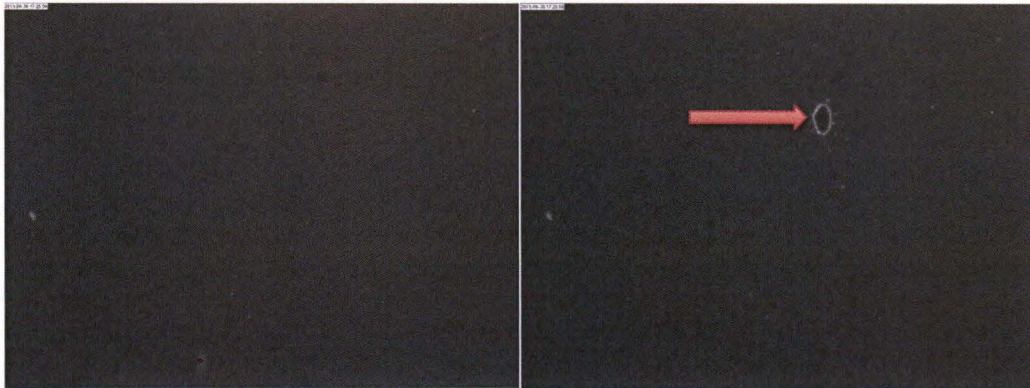


Fig. 3-5: The surface of the Al coated glass sample seen through the camera. On the left is the glass sample before the test. On the right is the same area on the sample, but with one area burned by the high power laser.

As we hinted previously, using ND filters can effectively avoid damages like this. For this set up, we tried several combinations of ND filters. All the ND filters we have in the lab are from Thorlabs. To obtain the signals, we first used a ND10A and a ND04A filter in series close to the pump laser source. We then removed the ND04A filter for a few second so to let the sample expose to a slightly stronger pump laser. After the short exposure, we put the ND04A filter back. We are doing this because we observed that with only ND10A filter, the pump laser power was so powerful that it burned the sample within a few seconds, while with both filters in series, the pump laser was not powerful enough and we could not observe any

signal on the oscilloscope. We are yet able to explain the reason behind this phenomenon.

Fig. 3-6 shows a typical view we would see on the oscilloscope during the experiment when we do get signals. All four channels are shown in the figure. Channel 1 (yellow) was connected directly to the pump laser, so it shows the pump laser pulses. In this specific test, the pump laser was tuned to a repetition rate of about 650Hz. Right in front of the sample, the total power of the pump and probe lasers was detected to be around 5.72mW, the pump laser only was detected to have 61.7 μ W of power, and the probe laser only had 5.60mW of power. Channel 2 and Channel 3 (indigo and purple) are the signals received by the two detectors in the balanced detector (the MONITOR+ and MONITOR -). Channel 4 (green) is the difference between Channel 2 and Channel 3. Notice that the image in Channel 4 was inverted in the oscilloscope.

To ensure that the signals we see in Channel 4 were not part of the pump signal, we only need to block the probe beam: if the signals in Channel 4 are merely caused by the pump pulses, we should still see these signals even without the probe beam. On the other hand, if these signals are what we are looking for, blocking the probe beam should make these signals disappear. When we blocked the probe beam, Channel 4 showed no signals—thus we confirmed that what we saw were not noise from the pump laser, and that the longpass filters installed on the balanced detector were effective.

Fig. 3-7 shows a close-up view of another test, with the pump laser tuned to a repetition rate of about 450Hz. We are going to use the data points stored from this test in the data analysis section.

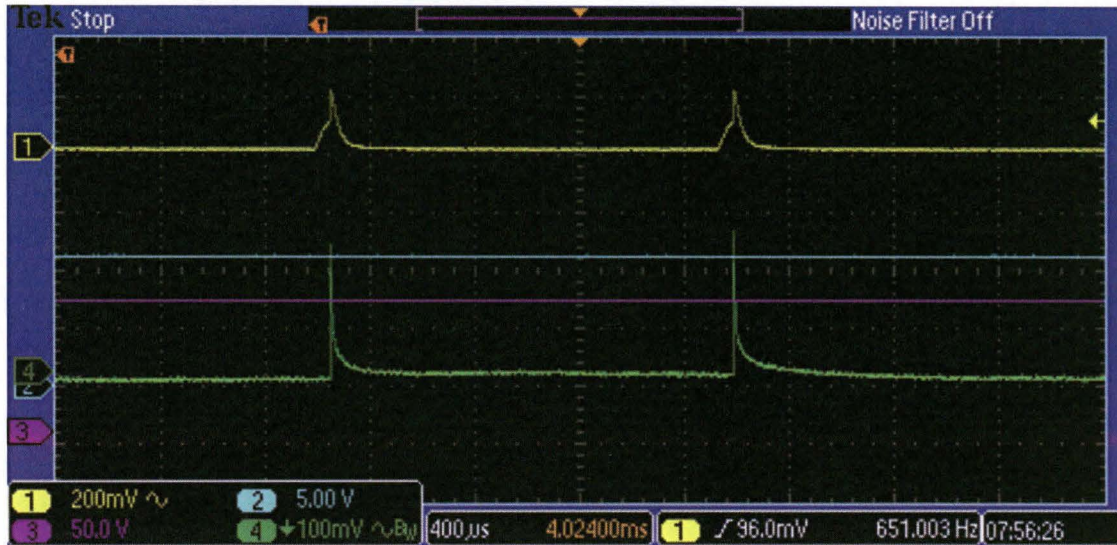


Fig. 3-6: Oscilloscope shows the detected signals collected in the pump-and-probe system. Channel 1 (yellow) was connected directly to the pump laser, so it shows the pump laser pulses. In this specific test, the pump laser was tuned to a repetition rate of about 650Hz. Channel 2 and Channel 3 (indigo and purple) are the signals received by the two detectors in the balanced detector (the MONITOR+ and MONITOR -). Channel 4 (green) is the difference between Channel 2 and Channel 3. Notice that the image in Channel 4 was inverted in the oscilloscope.

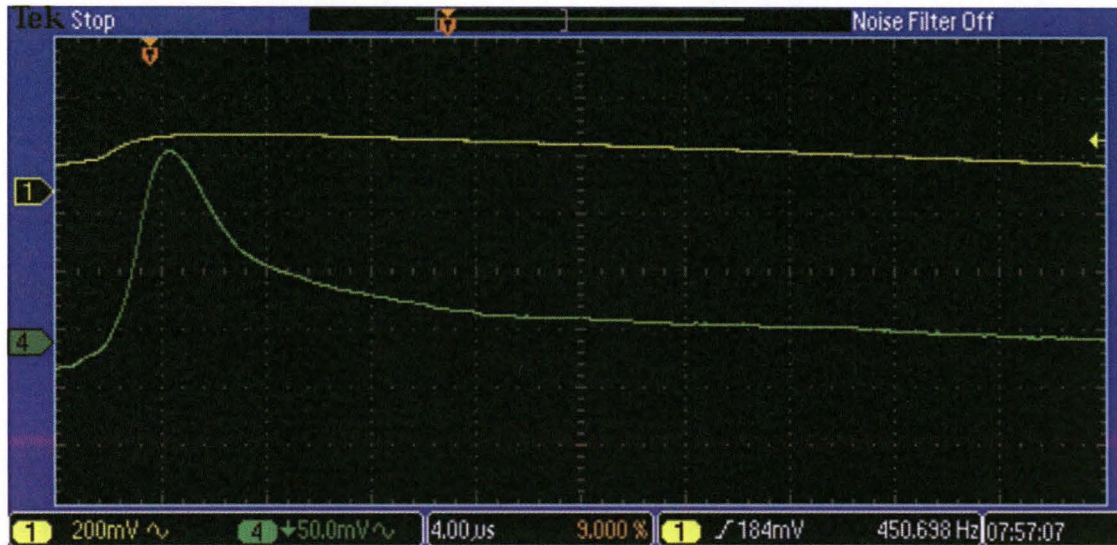


Fig. 3-7: A close-up view of one of the signals on the oscilloscope. Channel 1 (yellow) was connected directly to the pump laser. Channel 4 (green) is the difference between the output of MONITOR+ and MONITOR- on the balanced detector. Notice that the image in Channel 4 was flipped.

We saved the image and the data points in Channel 4 in a USB drive, and compared the data points against our simulation.

3.2 Simulation and Data Comparison

We simulate the cooling process (as the green curve shown in Fig. 3-7) with Matlab. The coding was previously done by Professor Minnich.

A typical simulated cooling curve looks like Fig. 3-8. The X axis is the time, in μ s, the Y axis is the temperature, in K.

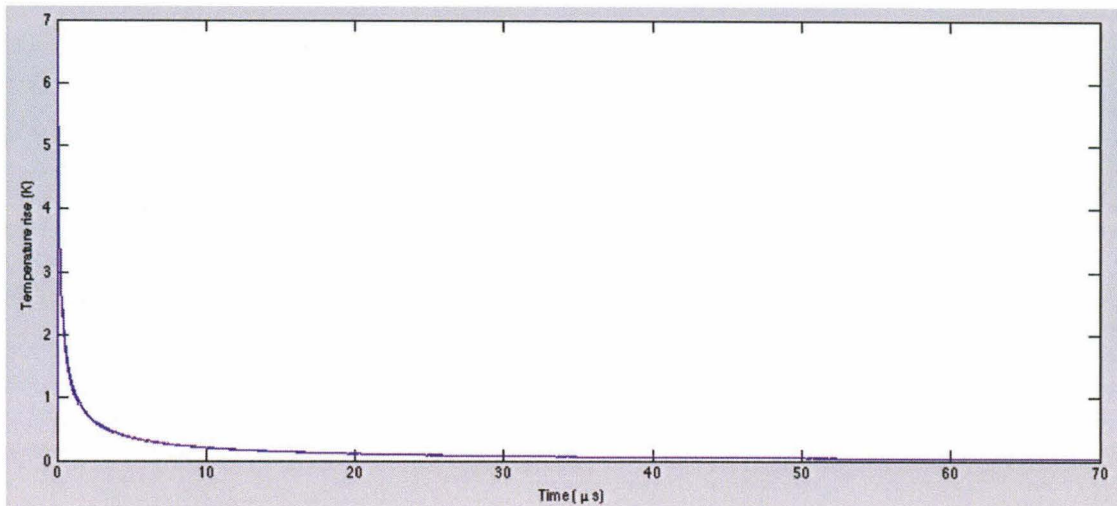


Fig. 3-8: A Matlab simulation result. The X axis is the time, in μs , the Y axis is the temperature, in K.

In Matlab, we are able to modify various parameters of the experiment. Among all, we studied the effects the following parameters had on the simulation: the thermal conductivity of the transducer and the substrate, the thickness of the transducer and the substrate, and the interface conductance (the interface between the transducer and the substrate). Given a specific experiment, we should know all the parameters except for the thermal conductivity of the sample, in which case we can easily compare the simulation against the experiment data by adjusting the thermal conductivity and watching the change in the cooling curve.

In our situation, the transducer is an Al film with a thickness of 100nm, the substrate is a 1mm thick layer of glass sample. In the simulation, we set the thermal conductivity of Al to be $237 \text{ Wm}^{-1}\text{K}^{-1}$, and that of glass to be $1.4 \text{ Wm}^{-1}\text{K}^{-1}$. Fig. 3-8 is the result of the simulation with the parameters we just assigned.

To compare the simulation result against the data points we collected from the oscilloscope, we plot the curves on the same graph. Fig. 3-9 shows the two curves in their original forms, and Fig. 3-10 shows the two curves after normalization. Notice that the solution is linear, so normalization will not change the shape of the curve.

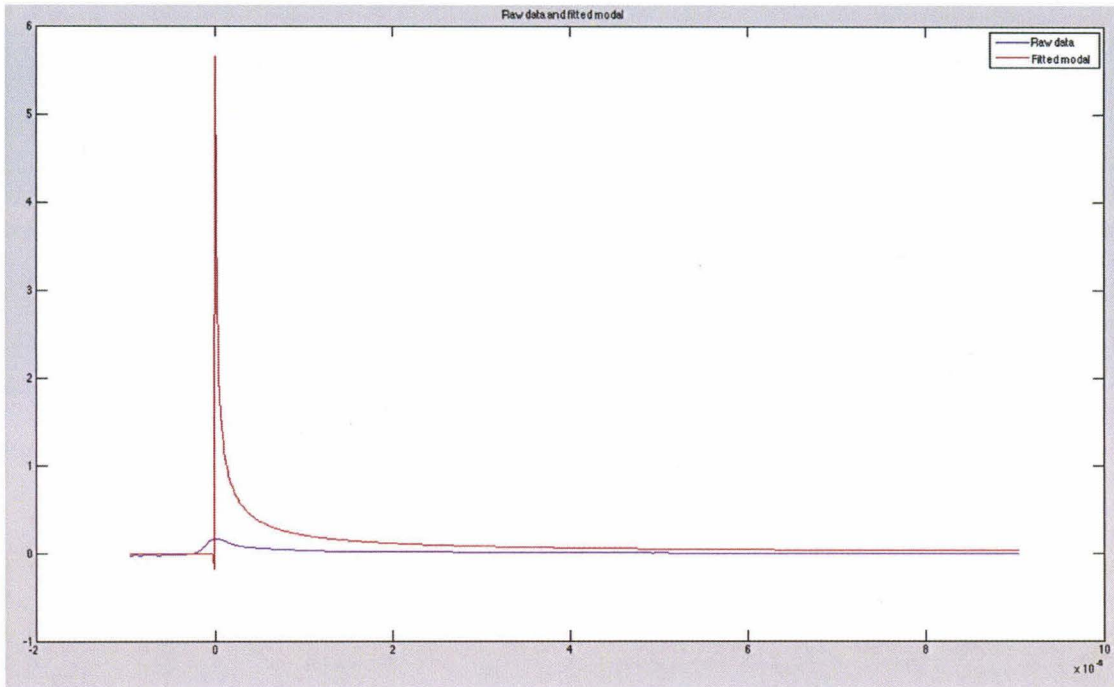


Fig. 3-9: Un-normalized curves. The red curve is the simulation result, and the blue curve is the experimental result.

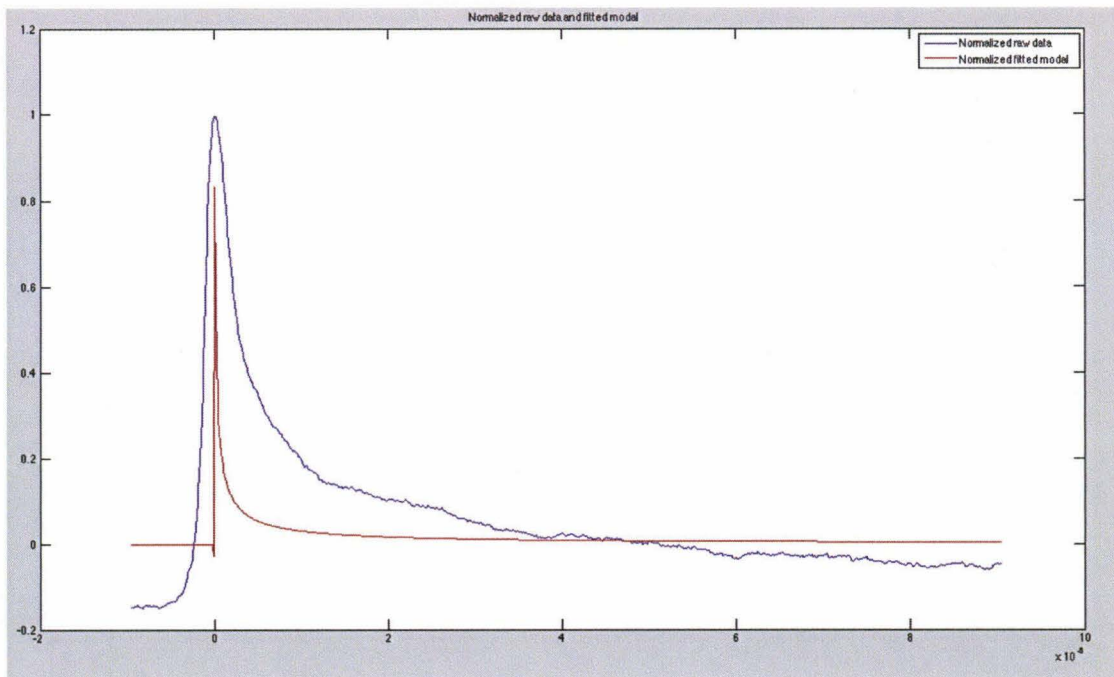


Fig. 3-10: Normalized curves. The red curve is the simulation result, and the blue curve is the experimental result.

In the experiment, we stored 100K data points. When we plotted the data points, we plotted one data point per every 100 points to get the final result faster. Thus, we have 1000 data points in each red and blue curve in Fig. 3-9 and Fig. 3-10. The reason that the normalized simulation result does not have a peak at 1 in the Y direction is also because we omitted 99 data points per every 100 points, and the peak happened to be omitted.

One thing to notice is that the blue curve does not have a sharp peak, as what we would find in the red curve. This is because the balanced detector we have in the experiment (Thorlabs PDB210A) has a bandwidth (3dB) of DC-1MHz, which means that sharp peaks like the one seen in the simulation will not be detected. We chose Thorlabs PDB210A because this set up was designed to measure ultralow thermal conductivity structures, instead of materials like glass, which has slightly higher thermal conductivity. If we were measuring a sample with a much lower thermal conductivity than glass, we should be able to detect the complete cooling curve.

Due to this reason, the experimental data we have collected from the glass sample is not quantitatively close to the simulation, even after normalization. But the cooling curves we have observed have qualitatively shown that the modified pump-and-probe system we designed and built is capable for measuring ultralow thermal conductivity structures like the nano-lattice.

Chapter 4

Summary and Outlook

4.1 Summary

We were inspired by the nano-lattice structure created by the Greer Group at Caltech to design and build an experimental apparatus that can measure ultralow thermal conductivity structures. We chose to modify the pump-and-probe method because with this technique we will be able to measure structures in microscopic scale without physical contacts. In Chapter 2, the design process and the implementation of the modified pump-and-probe system is described in details. Different from a typical pump-and-probe system, our set up has a pump laser with very low repetition rate (a few hundred Hz).

In this thesis, we did not run test on the nano-lattice sample created by the Greer Group, but instead, we measured a glass sample, and were able to quantitatively show that the modified pump-and-probe system is capable of measuring ultralow thermal conductivity structures. This experimental apparatus will be passed on to a PhD student in the Minnich Group, who will continue studying the ultralow thermal conductivity with the apparatus. Some improvements need to be made on the existing system before it can be used to measure ultralow thermal conductivity structures. Firstly, the CW probe laser needs to be chopped by an EOM to carry less energy. Secondly, the chopped probe laser needs to be synchronized with the pump laser pulses, so that each probe laser pulse arrives slightly later after each pump laser pulse. Thirdly, the laser power at the sample needs to be controlled more carefully, because the lower the thermal conductivity the sample

possesses, the easier it is for the heat to accumulate in the transducer and to be damaged by the heat.

In Chapter 3, we presented the results from one of the tests we did on a glass sample, as well as a simulation. We were not able to quantitatively fit the data points we obtained from the experiment to the simulation, because the bandwidth of the balanced detector was too small (yet big enough for samples with lower thermal conductivity than glass) to detect the peak of the cooling curve. However, the signals we detected qualitatively show that our experimental apparatus has the capability of measuring ultralow thermal conductivity structures, such as a nano-lattice.

4.2 Outlook and Conclusion

While we have designed and built an experimental apparatus that is capable of measuring ultralow thermal conductivity structures, we have yet measured any nano-lattice sample. In the past few months, the Greer Group made some new improvements on the nano-lattice structure. One of the important improvements they made was designing and writing a plate on the top of the lattice structure (as shown in Fig. 4-1). The plate will serve as a good supporting stage for the Al transducer, and will also allow the heat to transfer into the lattice structure more easily. The sample shown in Fig. 4-1 was coated with ALD niobium doped titania (Nb doped TiO_2). The niobium makes the structure more conductive so it's easier to see in an SEM.

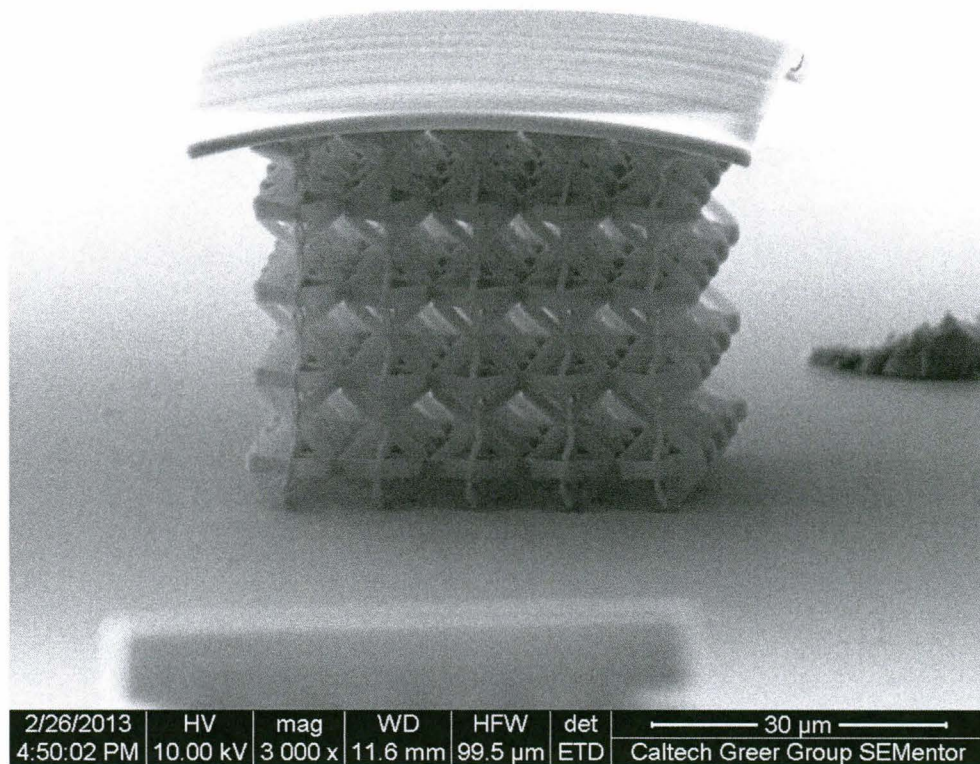


Fig. 4-1: Nano-lattice structure with a planer structure on the top. The plate will serve as a good supporting stage for the Al transducer, and will also allow the heat to transfer into the lattice structure more easily. Credit: Greer Group at Caltech.

Another direction we can go into with this experimental apparatus is to study the conductivity of the super nano-lattice, which is a nano-lattice structure with alternating material coating. We have already known from previous studies that planer superlattices with alternating layers of different materials possess very low thermal conductivity due to the thermal resistance of numerous interfaces. Similarly, if we coat the nano-lattice structure with alternating materials, we expect its thermal conductivity to drop even further. With the experimental apparatus built in the thesis, we will be able to measure the thermal conductivity of the super nano-lattice.

Not only the nano-lattice, many other materials with ultralow thermal conductivity can also be measured with our modified pump-and-probe system. The study of ultralow thermal conductivity, especially in micro and nano scale, can be important for many research fields. Once we are able to study the thermal properties of materials in nano scale, we will be able to look at materials from a whole new perspective, and many new materials with desirable properties will be made possible.

Bibliography

- [1] <http://onlinelibrary.wiley.com.clsproxy.library.caltech.edu/doi/10.1002/adfm.201201285/abstract>. Accessed on May 7th, 2013.
- [2] T. A. Schaedler, A. J. Jacobsen, A. Torrents, A. E. Sorensen, J. Lian, J. R. Greer, L. Valdevit, W. B. Carter. Ultralight Metallic Microlattices. *Science* 334 (6058), 962-965 (2011)
- [3] http://www.engineeringtoolbox.com/thermal-conductivity-d_429.html. Accessed on May 6th, 2013.
- [4] <http://en.wikipedia.org/wiki/Aluminium>. Accessed on May 7th, 2013.
- [5] W. S. Capinski, H. J. Maris. Improved Apparatus for Picosecond Pump-and-probe Optical Measurement. *Rev. Sci. Instrum.* 67, 2720 (1996); doi: 10.1063/1.1147100
- [6] A. J. Schmidt. Optical Characterization of Thermal Transport from the Nanoscale to the Macroscale, May 2008.
- [7] D. G. Cahill. Analysis of heat flow in layered structures for time-domain thermoreflectance. *Rev. Sci. Instrum.* 75, 5119 (2004); doi: 10.1063/1.1819431
- [8] A. F. Mills. *Basic Heat and Mass Transfer*. Prentice Hall, c1999.
- [9] <http://refractiveindex.info/?group=METALS&material=Aluminium>. Accessed on May 7th, 2013.
- [10] http://www.thorlabs.us/NewGroupPage9.cfm?objectgroup_id=1299. Accessed on May 6th, 2013.